WESTERN REGION TECHNICAL ATTACHMENT
NO. 99-17
AUGUST 24, 1999

A CASE STUDY OF A WIND EVENT IN THE PALM SPRINGS REGION

Ivory J. Small and Akriti Shah
NWSO San Diego, CA

[Note: Appendices and Figures appear on web page only.]

Introduction

In the mountainous Palm Springs (PSP) region at 0000 UTC 17 June 1998, westerly winds were gusting from 30 to near 50 knots at the ridge tops and on the leeward side of the San Jacinto Mountains (Fig.1). These winds produced dust storms that reduced visibility. Blowing dust and sand resulted in a road closure in the Palm Springs area, and small aircraft were also affected. The winds are often created by several synoptic and orographic features in the region. The features are the surrounding complex terrain, the coast to desert pressure gradient flow, and the synoptic scale cross-barrier flow near the mountaintops. In addition, on this particular day there was an enhanced inversion due to a Catalina Eddy (Clark and Dembek, 1990). In order to determine the phenomena which caused these winds in the Palm Springs region an analytical, computational, and case comparison approach was used. After some background information on wind influenced by mountainous terrain is given, the case comparison will be presented and analyzed. (Some of the wind reports used in this study were provided by the South Coast Air Quality Management District (SCAQMD). Values for U = mean wind, N = Brunt-Vaisala frequency, and H = obstacle height were obtained from the 0000 UTC 17 June 1998 NKX sounding in order to calculate the Froude number F = U/NH. By using the available terms from the Froude calculation, the Scorer Parameter (see appendix B) was computed and physically analyzed. Finally, a summary and conclusion will be given.

Background Information on Wind Influenced by Mountainous Terrain

It has been long known that airflow is commonly more disturbed over mountainous terrain than over level country (Corby, 1954). Disturbances due to mountains can be broken down into two categories: 1) thermally induced winds; 2) terrain influenced winds such as mountain waves and mountain gap winds. Slope and valley wind systems are local, thermally driven circulations that form frequently in complex terrain areas (Whiteman,

1998). Winds can also blow from areas with lower air temperatures to areas of higher temperatures. Compensatory or return circulations higher in the atmosphere close the circulations , which form at the scale of heating. Stratified air flowing over mountainous terrain often generates atmospheric internal gravity waves or mountain waves (Keller, 1998). In order to describe wave amplification downstream from a mountain at different levels the Scorer Parameter is used. The Scorer Parameter is dependent on vertical wind shear and stability. It can determine whether a wave is an external or internal wave. Also the Froude number is used to examine flow characteristics in mountainous terrain.

Gap winds can be defined as the flow of relatively homogenous air in a sea level channel or mountain valley with a source region or reservoir at one end (Reed, 1931). The speed and depth of gap wind flow is strongly controlled by topography and stability. Mountain ranges act to divide contrasting air masses, enabling large sea-level pressure gradients to develop (Macklin et al., 1988). Strong ageostrophic winds can occur in coastal gaps or channels when the approach of a synoptic scale disturbance generates an along-channel pressure gradient. This scenario is often observed in gaps along the mountainous coasts of the eastern Pacific and Gulf of Alaska (Overland and Walter, 1981). The Froude number can be used to examine gap wind flow.

To better understand the flow over an obstacle or mountain, Durran (1990) describes the dynamics of a homogeneous fluid flowing over a ridge-like obstacle using Fig. 2. The assumption is that the flow is in hydrostatic balance and bounded by a free surface. Using the shallow-water momentum and continuity equations, the Froude number (Fr), is defined as the ratio of the fluid velocity to the speed of linear shallow water gravity waves. $Fr^2 = u^2/gD$. For $Fr > 1$ (supercritical flow), the height of the fluid rises and slows down as it crosses the top of an obstacle, reaching its minimum speed at the crest, and then collapses and accelerates on the leeward side. For the case $Fr < 1$ (subcritical flow), the fluid thins and accelerates as it crosses the top of the obstacle, reaching its maximum speed at the crest. In the last case, that explains downslope windstorms, the subcritical fluid flow on the windward side of the obstacle thins and accelerates, eventually becoming supercritical at the top of the obstacle. The fluid continues to accelerate on the leeward side. Finally the flow undergoes a hydraulic jump to conform to the ambient downstream conditions (Durran, 1990).

Case Comparison and Results

a. Gulf of Tehuantepec Case

Steenburgh et al., (1998) investigated the structure and evolution of gap flow through Chivela Pass and over the Gulf of Tehuantepec, Mexico on 12-14 March 1993 (Fig. 3a). The surge of cold air through the gap was part of a cold front associated with a deepening mid-latitude cyclone over the Northern Gulf of Mexico. A strong cross-barrier pressure

gradient had developed over Chevela Pass (Fig. 3b). Northerly flow resulted in strong gap outflow winds from the Gulf of Mexico, through the pass, and out over the Gulf of Tehuantepec. The sounding in figure 4a. showed a westerly flow aloft. However, there is strong northerly flow throughout much of a surface-based layer of increased static stability (the inversion on the 0000 UTC 13 March 1993 raob was the strongest). A north-south vertical cross section (Fig. 4b) from the mesoscale model showed that over and immediately downwind of Chevela Pass a wavelike undulation and leeside subsidence was evident. This suggests that the mountains surrounding the pass had excited a mountain wave. However, the gap flow was the dominant factor in accelerating the flow.

b. Palm Springs Region Case

At 1200 UTC 16 June 1998, the 500 mb height and vorticity (Fig. 5a) showed an upper-level trough of low pressure moving toward Nevada. This serves to increase the upper-level cross-barrier flow. A Catalina Eddy was in progress, and the clouds were thick enough for drizzle and light rain in some location. The Catalina Eddy can be clearly identified as a cyclonic flow in the low clouds on the 1800 UTC 16 June 1998 visible satellite imagery (Fig. 5b). Fingers of cloudiness can be seen extending into the major mountain passes, including Banning Pass (the gap between the San Bernardino and San Jacinto Mountains in Fig. 1) northwest of Palm Springs. The Catalina Eddy circulation can also be seen via a southerly flow along the coast in the 1800 UTC 16 June 1998 surface plot (Fig. 5c). As a result of the temperature and resulting pressure contrast between the cooler high pressure region near the coast and the warmer low pressure region in the desert, the sea breeze extends through the passes and into the deserts. The surface map in Fig. 6a and Fig.6b shows a strong along-channel pressure gradient, similar to that seen in the Gulf of Tehuantepec case, enhanced via development of a rather deep (995 mb) surface low over southern Nevada. The 2100 UTC cross-barrier pressure gradients from LAX to DAG, LAX to TRM, and SAN to IPL were 11.9 mb, 9.1 mb, and 9.2 mb respectively. [West to east (onshore) pressure gradients of 0 - 3.9 mb, 4.0 - 6.9 mb, and 7.0 mb and over are considered weak, moderate, and strong pressure gradients respectively for those particular cross-barrier gradients]. The 2100 UTC cross-barrier pressure gradient from LAX to southwestern Nevada (TPH) was 9.3 mb. (It is important to notice, via comparison of the graphics and the actual values, that the actual pressure gradients are stronger than they appear on these AFOS graphics. This is a point to keep in mind when viewing pressure gradient contours on the longer-range coarse resolution graphics).

A temperature inversion was present on the 0000 UTC 17 June 1998 NKX sounding in Fig. 6c (as was seen on the 0000 UTC 13 March 1993 sounding in the Gulf of Tehuantepec case). There were winds of about 10 knots near the surface, and stronger winds of up to 30 knots aloft. The flow of cool marine air enhanced by the Catalina Eddy had produced the strong capping inversion. Much like the Gulf of Tehuantpec case, the northwesterly gap outflow wind in the Palm Springs region was primarily due to its location with respect to Banning Pass.

Figure 7a, Fig. 7b, Fig. 8a, and Fig. 8b for 1200 UTC, 1800 UTC, 2100 UTC, on 16 June, 1998 and 0000 UTC 17 June 1998 respectively show the progress of the event. Notice the calm wind at PSP at 1200 UTC in Fig. 7a. By 0000 UTC 17 June 1998 the observed wind gusts were up to between 30 and 50 knots in some mountain and desert locations.

Winds further south on the lee side of the mountains were characteristic of mountain waves. This was likely due to less blocking from a smaller mountain range as well as the absence of a gap in the mountain range for gap winds to develop. Pilot reports indicating 1000 feet per minute up and downdrafts supported the presence of mountain wave activity (Appendix A).

Computations

Other supporting evidence of mountain wave activity are calculations of the Froude number and Scorer Parameter. The relationship between the Scorer Parameter (with the assumption that curvature can be neglected) and vertically propagating waves can be found in Appendix B. The relation that must be satisfied for vertically propagating waves is $k^2 < N^2/U^2$ or $k < N/U$.

For simplicity, it is assumed that the frequency of the lee wave is generated by sinusoidal topographic features of wave number k. [The wave number $k = 1/\lambda$ where λ = the wavelength of the mountain (Holton, 1979)].

Thus, vertical propagation is possible if $k < N/U$ is satisfied. Stable stratification, wide mountains, and comparatively weak zonal flow provide favorable conditions for vertically propagation waves. Of course the equation $k< N/U$ was obtained from conditions of constant basic state flow. In reality both the zonal wind U and the stability parameter N generally vary with height. Under certain conditions (e.g., an intense inversion just above the mountain top) large amplitude waves can be formed which may generate severe downslope surface winds and zones of strong clear air turbulence (Holton, 1979). This potential is clearly seen in the observations as well as the pilot reports in appendix A.

When using values from the 0000 UTC 17 June 1998 NKX sounding

$N = 1.48 \times 10^{-2}\ s^{-1}$
$U = 5$ m/s

and approximating the wavelength of the mountain barrier as 50 km (50000 m) to determine k

$k = 2.00 \times 10^{-5}\ m^{-1}$

the relationship yields

$2.00 \times 10^{-5} < 2.96 \times 10^{-3}$

Therefore, the Scorer Parameter reveals a case of internal gravity waves since in this case $k < N/U$.

The Froude number calculated using an alternate form of the Froude number, $F = U/NH$, (with U and N values from the Scorer Parameter calculation , and an average mountain height of H = 1525 m from the sounding) results in a value of F = 0.18. [It is interesting to note that the N value of 1.48×10^{-2} s^{-1} calculated for this Catalina Eddy case is very close to the 2×10^{-2} s^{-1} value used in the Clark and Dembek (1991) Catalina Eddy event]. Since the value is less than 1, it suggests a subcritical flow. This means significant blocking was present resulting in gap flow through the Banning Pass. Concluding, both a mountain wave and gap winds were present.

Summary and Conclusion

We have seen that complex terrain can result in a very complex flow pattern in the Palm Springs region. The parameters evaluated in this Technical Attachment support gap flow as well as mountain wave activity in the area. Pilot reports of up and downdrafts of 1000 feet per minute in the area also serve to support the presence of mountain wave activity. Another interesting point is that even though the surface pressure gradients were very strong, the winds would only be considered moderate for those areas (assuming, in general, gusts of 0 - 29 knots, 30 - 49 knots, and 50 knots or greater would be considered weak, moderate, and strong winds respectively in the mountains and deserts). Also with stronger upper-level support [stronger 850 mb, 700 mb, and 500 mb height gradients (Small, 1995) along with a stronger thermal gradient at those levels], the winds could have been increased into the strong category.

Even though studying this Southern California wind event has provided more knowledge of wind interaction with topography, more data are needed and more study is required. The scarce amount of desert wind recording stations made it difficult to observe wind behavior on the leeside of the mountain range. More studies in this area will provide us with better knowledge of wind behavior that can be applied to many other similar regions.

Acknowledgments

We would like to thank Dr. Scot Rafkin from SJSU for his assistance and guidance, and the South Coast Air Quality Management District (SCAQMD) for their archived data of the Los Angeles basins winds and temperature data. Also we would like to thank Dimitra Boucouvala for providing the Southern California map used for plotting data.

References

Clark, H. E., and S. R. Dembek, 1990: The Catalina Eddy event of July 1987: A coastally trapped mesoscale response to synoptic forcing. *Mon. Wea. Rev.*, **119**, 1714-1735.

Corby, G. A.., 1954: The airflow over mountains - A review of the state of current knowledge. *Quart. J. Roy. Meteor. Soc.*, **80**, 491-521

Durran, D. R., 1990: Mountain waves and downslope winds. Atmospheric process over complex terrain. William Blumen, Ed., *American Meteorological Society Monographs., 23* **No. 45**, 59-81.

Holton, J. R., 1979: *An Introduction to Dynamic Meteorology*, Second Edition. Academic Press Inc. 391 pp.

Holton, J. R., 1992: *An Introduction to Dynamic Meteorology*, Third Edition. Academic Press Inc. 511 pp.

Keller, T. L., 1998: Mountain waves and windstorms. National Center for Atmospheric Research, Boulder, CO, 18 pp.

Macklin, S. A.. et al., 1988: Offshore-directed winds in the vicinity of Prince Williams Sound, Alaska. *Mon. Wea. Rev.*, **116**, 1289-1301

Overland, J. E. and B. A. Walter, 1981: Gap winds in the Strait of Juan de Fuca. *Mon. Wea. Rev.*, **109**, 2221-2233

Reed, T. R., 1931: Gap winds in the Strait of Juan de Fuca. *Mon. Wea. Rev.*, **59**, 373-376.

Small, I. J., 1995: Santa Ana winds and the fire outbreak of Fall 1993. NOAA Technical Memorandum NWS WR-230, 15 pp.

Steenburgh, W. J., D. M.. Schultz, and B. A. Colle, 1998: The structure and evolution of gap outflow over the Gulf of Tehuantepec, Mexico. *Mon. Wea. Rev.*, **126,** 2673-2691

Whiteman, C. D., 1998: Thermally driven wind systems. Battelle Pacific Northwest Laboratories, Richland, WA. 32 pp.

____, 1990: Observations of thermally developed wind systems in mountainous terrain. Atmospheric process over complex terrain. William Blumen, Ed., *American Meteorological Society Monographs., 23* **No. 45**, 5-42.

APPENDIX A

I. SELECTED PILOT REPORTS
(Turbulence reports indicated in bold type)

PSP UUA /OV PSP/TM 2011/FL010/TP C550/**TB SVR 010-030 MDT 030-085 LGT CHOP 085-120**

RAL UA /OV L35/TM 2148/FL008/TP PA28/**TB MDT/RM PILOT SAID RUFF TURBC ON FINAL BIG BEAR**

PSP UA /OV PSP-JLI 115020/TM 2225/FL105/TP P28R/SK CLR/**TB DURC PSP MDT MSTLY SMTH ABV 040/RM 20 SE JLI 1000 FPM UDDFS**

PSP UUA /OV PSP/TM 2258/FL050/TP C500/**TB MDT-SVR/RM DURGC SFC-050**

CRQ UA /OV JLI 115010/TM 2302/FL110/TP C180/SK CLR/**TB CONT LGT-BRF MDT UDDFS 1000 FPM 095-120**

APPENDIX B

I. The relationship between the Scorer Parameter and vertically propagating waves.

If U (cross-barrier flow) and N (stability) are allowed to vary in height (Holton, 1992), then the equation describing the motion is

$$(\partial^2 W'/\partial X^2 + \partial^2 W'/\partial Z^2) + L^2 W' = 0 \qquad (1)$$

where

$$L^2 = N^2/U^2 - 1/U \; d^2U/dZ^2 \qquad (2)$$

For simplicity, assume U = constant

$$L^2 = N^2/U^2 \qquad (3)$$

Also from (Holton, 1992) the condition for vertical propagation was

$$k^2 < L^2 \qquad (4)$$

Combining equations 3 and 4

$$k^2 < N^2/U^2 \qquad (5)$$

or

$$k < N/U \qquad (6)$$

is the condition that satisfies the requirement for vertically propagating waves to occur.

In Holton (1979), equation 5 is rearranged to

$$U < N/k \qquad (7)$$

For simplicity, it is assumed that the frequency of the lee wave is generated by sinusoidal topographic features of wave number k (wave number $k = 1/\lambda$ where λ = the wavelength of the mountain).

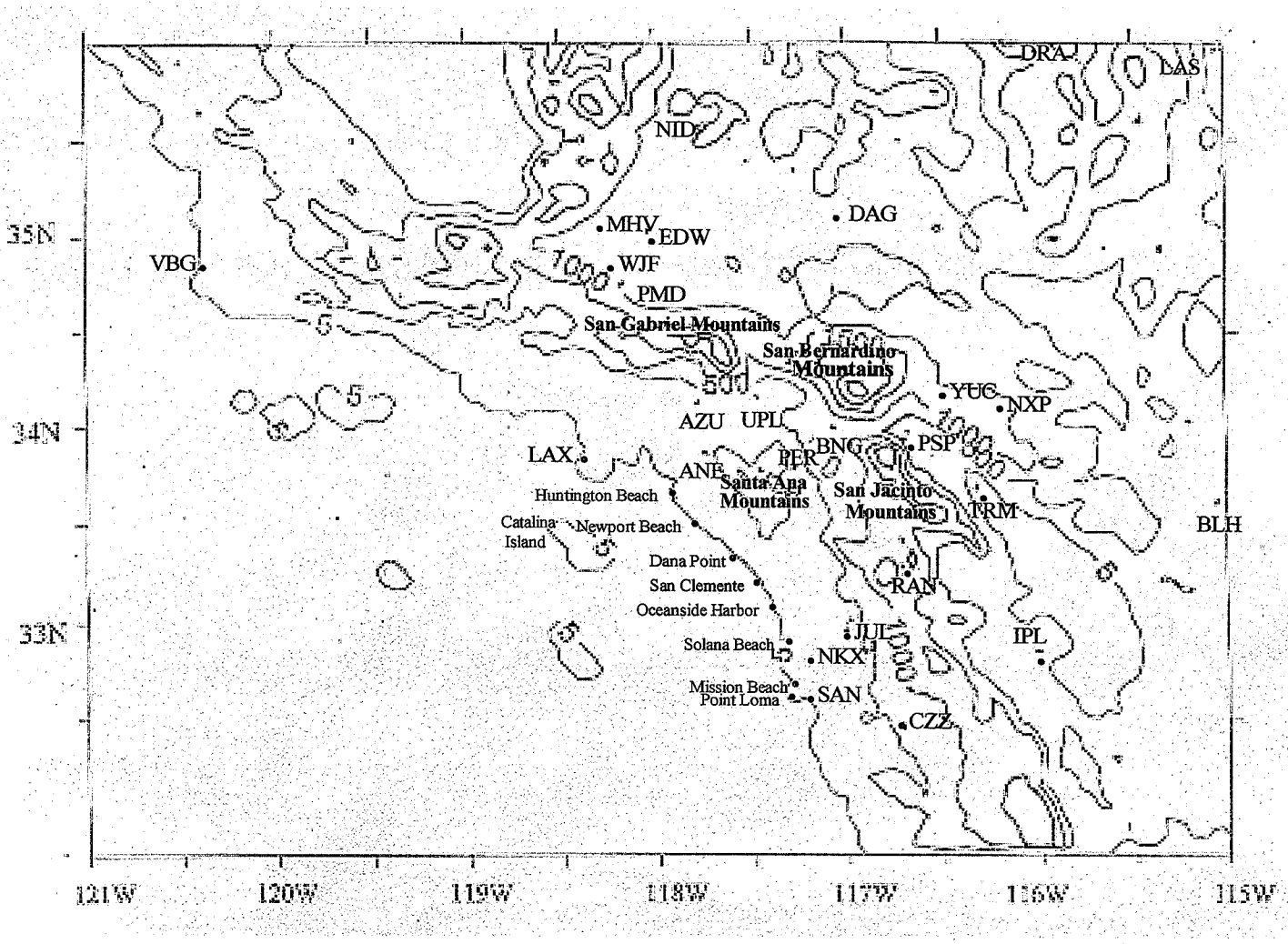

Fig. 1. Map of Southern California Terrain (Heights in meters).

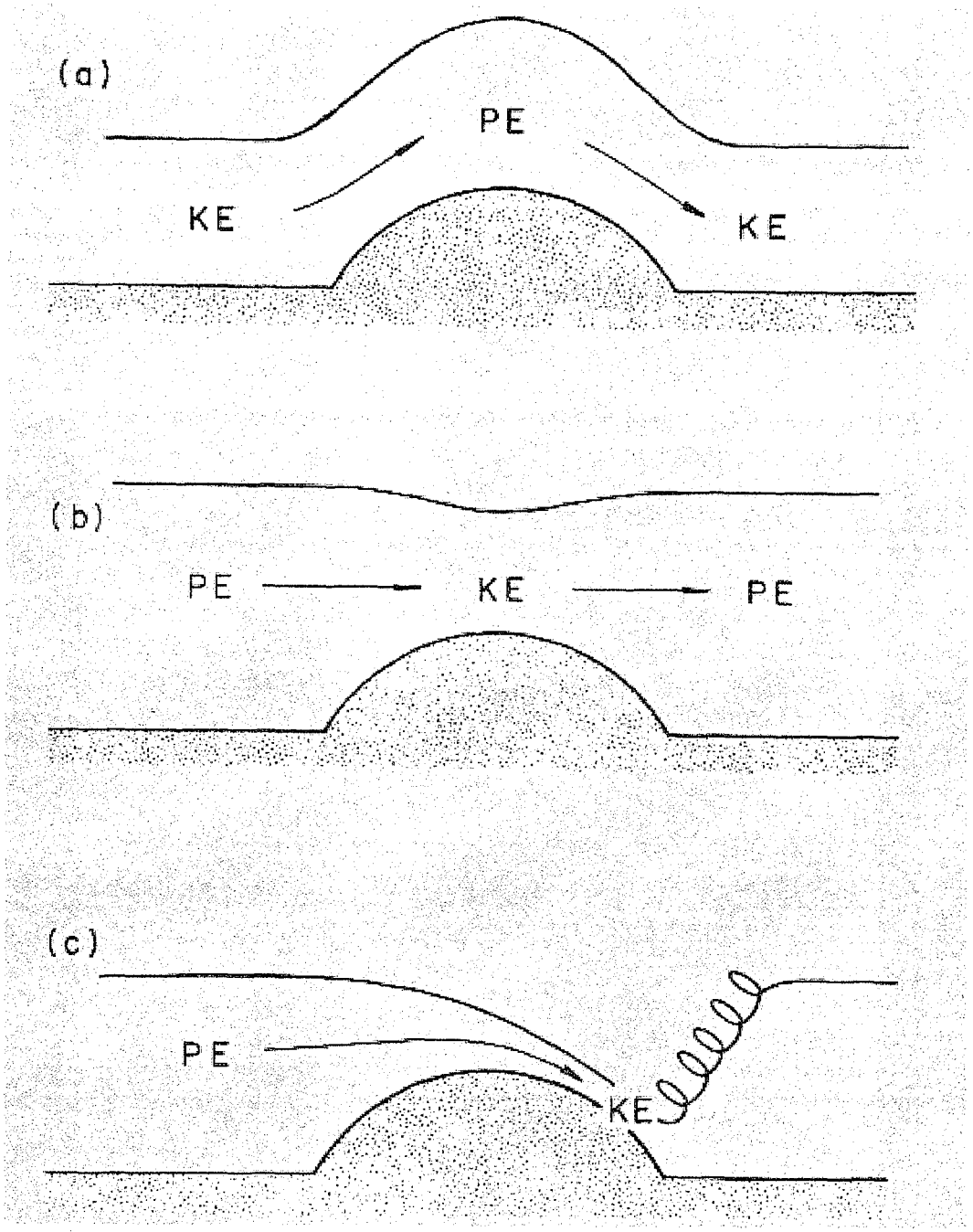

Fig. 2. Behavior of shallow water flowing over an obstacle: (a) everywhere supercritical flow, (b) everywhere subcritical flow, (c) hydraulic jump (After Durran, 1990).

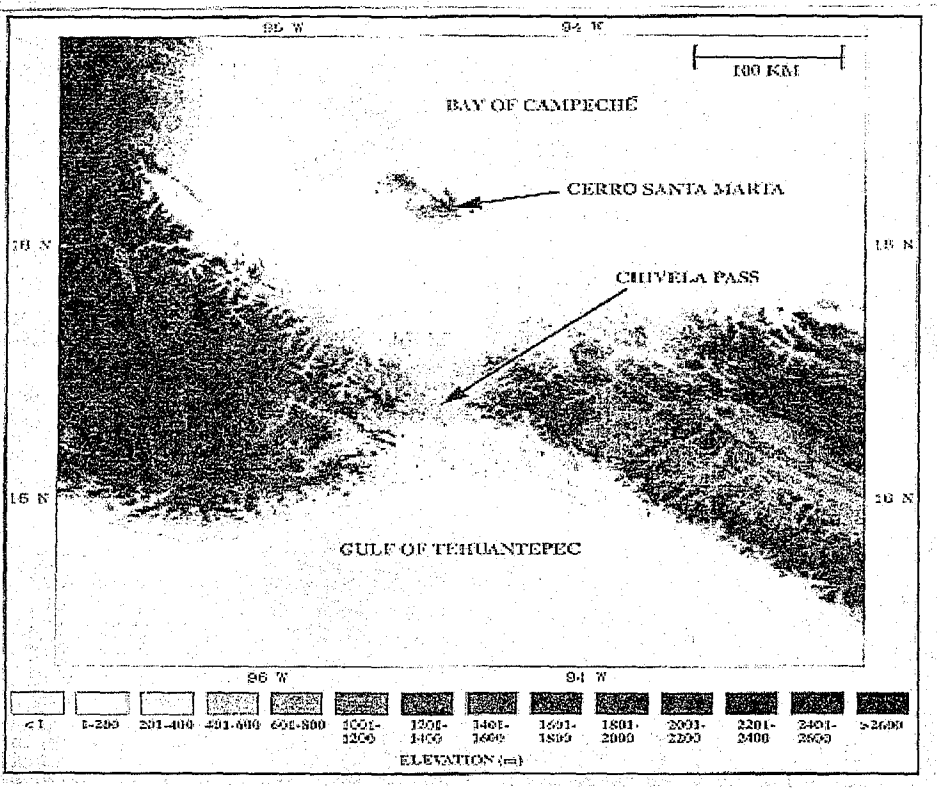

Fig. 3a. Terrain map of the Chivela Pass area of Mexico and South America (after Steenburgh et al. 1998) .

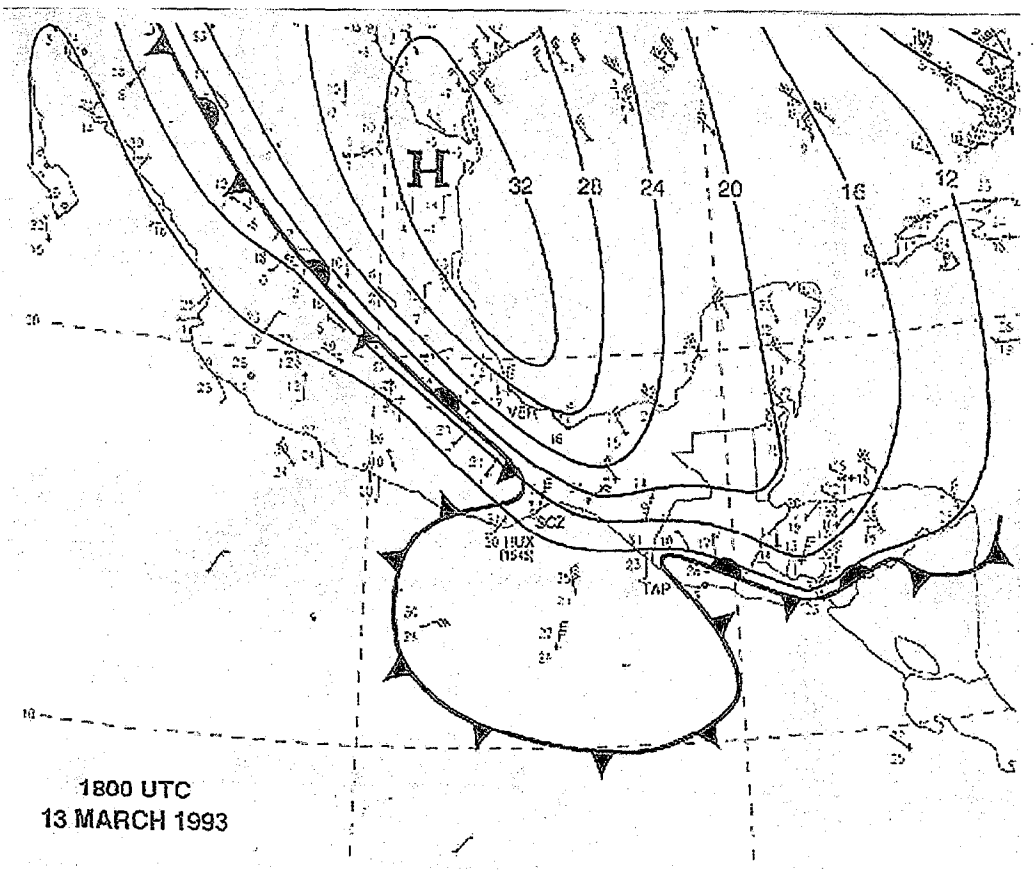

Fig. 3b. Manually analyzed surface map at 1800 UTC 13 March 1998. Solid lines are sea level pressure every 4 mb. Winds: one pennant, full barb, half-barb, and circle denote 25 m s^{-1}, 5 m s^{-1}, 2.5 m s^{-1}, and less than 1.25 m s^{-1} respectively (after Steenburgh et al. 1998) .

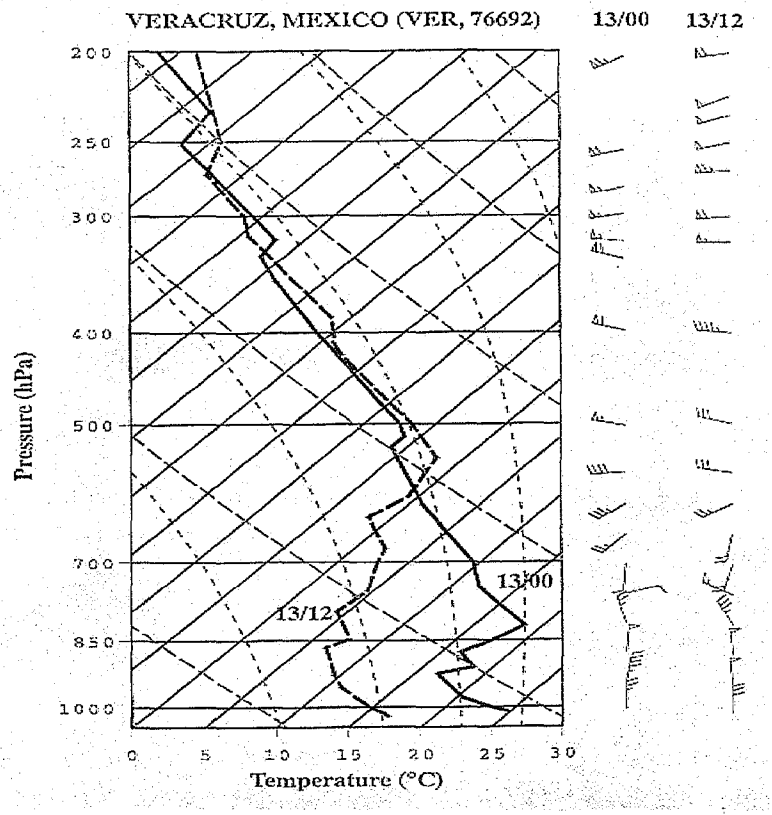

Fig. 4a. Temperature and wind profiles from Veracruz, Mexico (VER) at 0000 UTC 13 March and 1200 UTC 13 March. Wind conventions as in figure 3b (After Steenburgh et al. 1998).

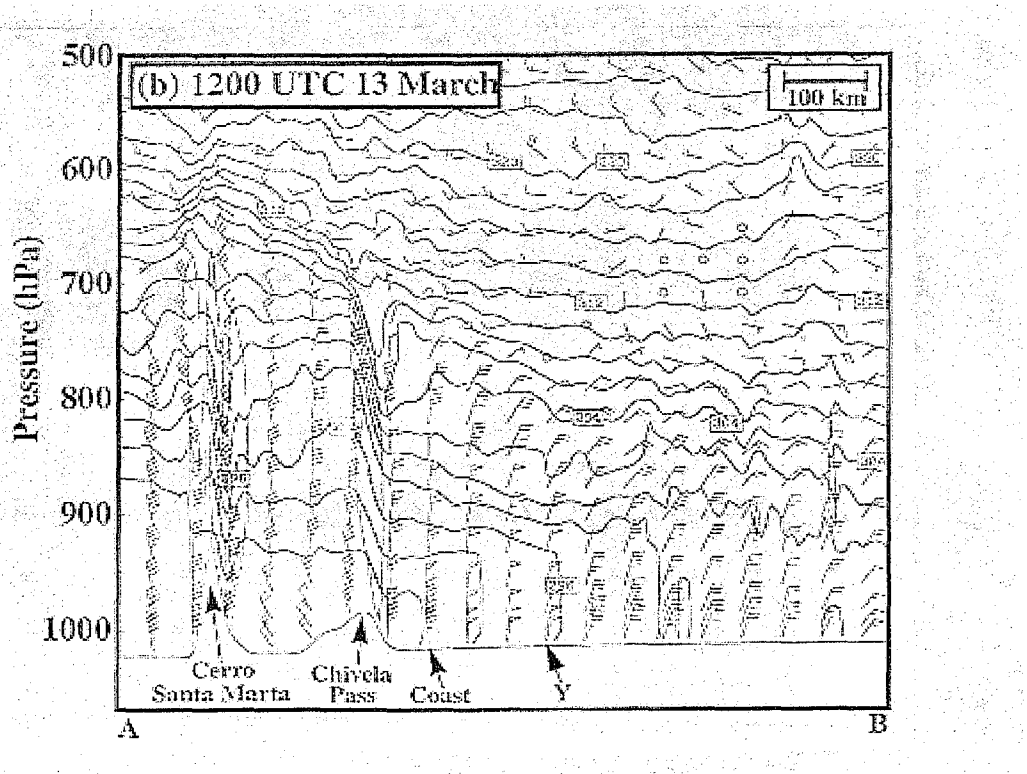

Fig. 4b. Cross section of potential temperature (every 2 K) and horizontal wind along a north-south line through Chivela Pass. Wind conventions as in Fig. 3b. Light (dark) shading identifies regions of rising (sinking) motion exceeding 3×10^{-1} m s^{-1} in magnitude (After Steenburgh et al. 1998).

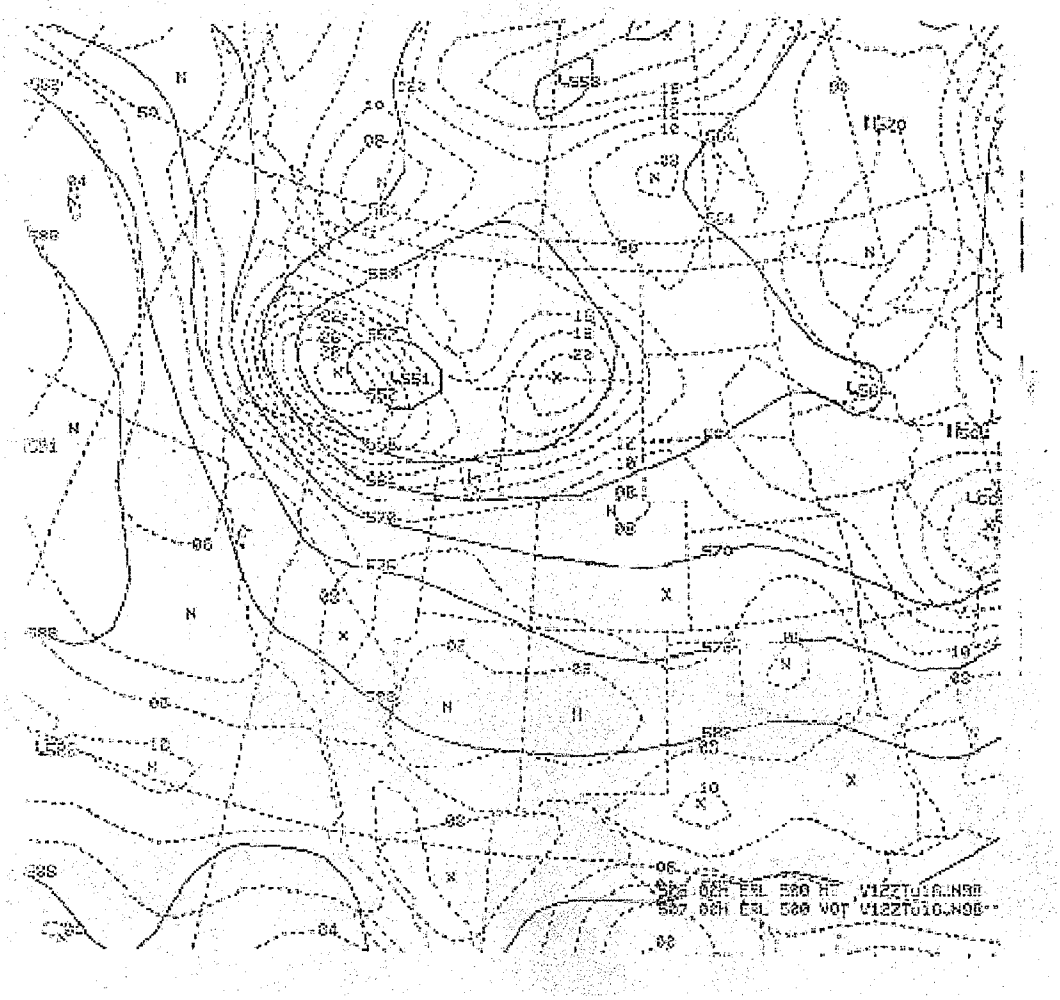

Fig. 5a. 1200 UTC 16 June 1998 500 mb Height and vorticity.

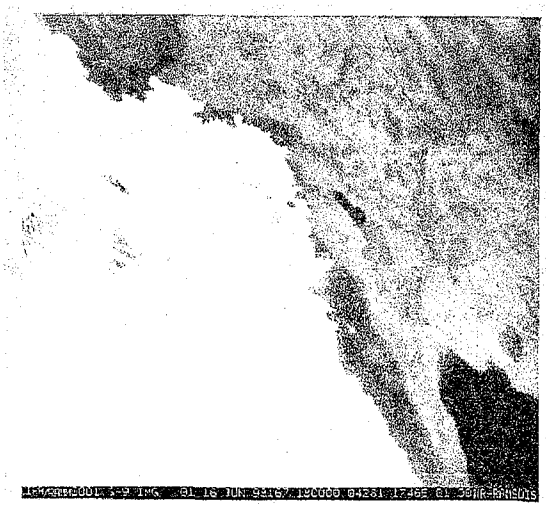

Fig. 5b. 1800 UTC 16 June 1998 visible satellite imagery.

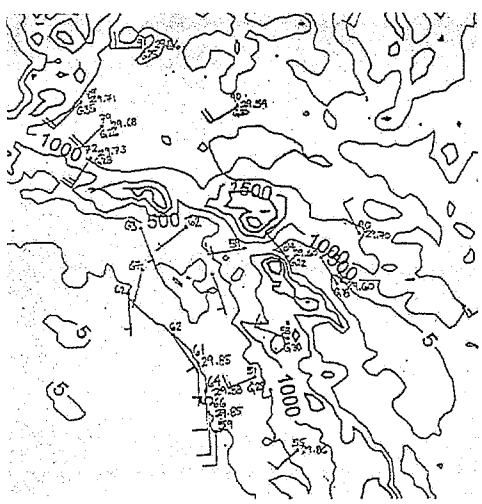

Fig. 5c. 1800 UTC 16 June 1998 Surface plot. Winds speeds in knots.

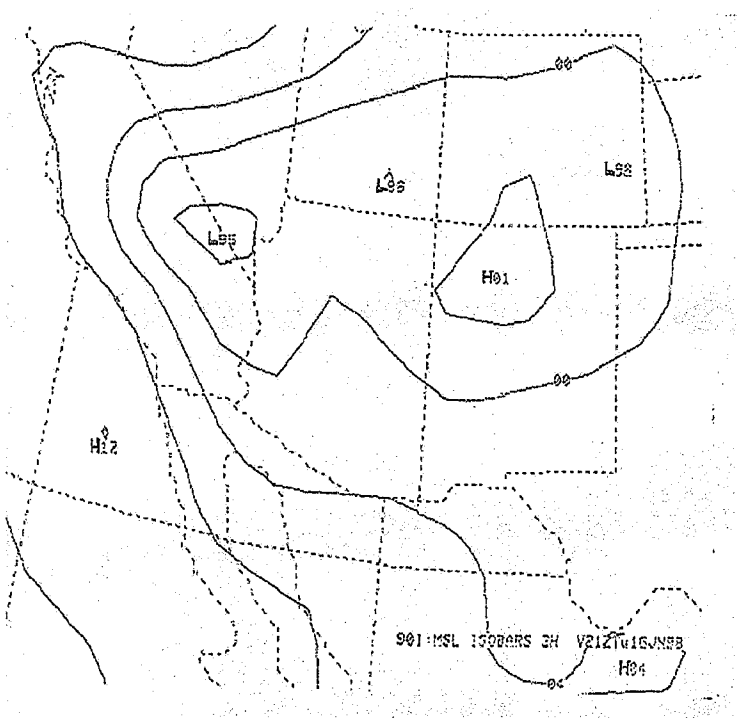

Fig. 6a. 2100 UTC 16 June 1998 surface map. Solid lines are sea level pressure every 4 mb.

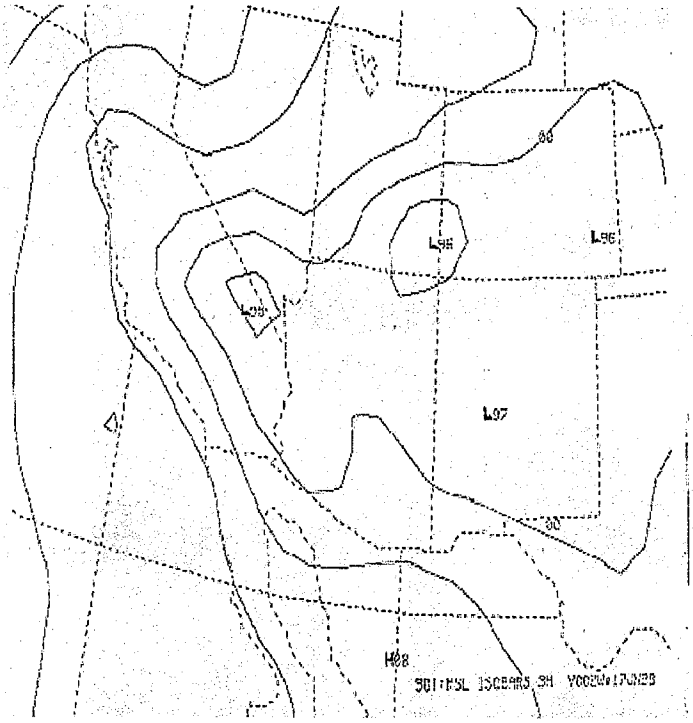

Fig. 6b. 0000 UTC 17 June 1998 surface map. Solid lines are sea level pressure every 4 mb.

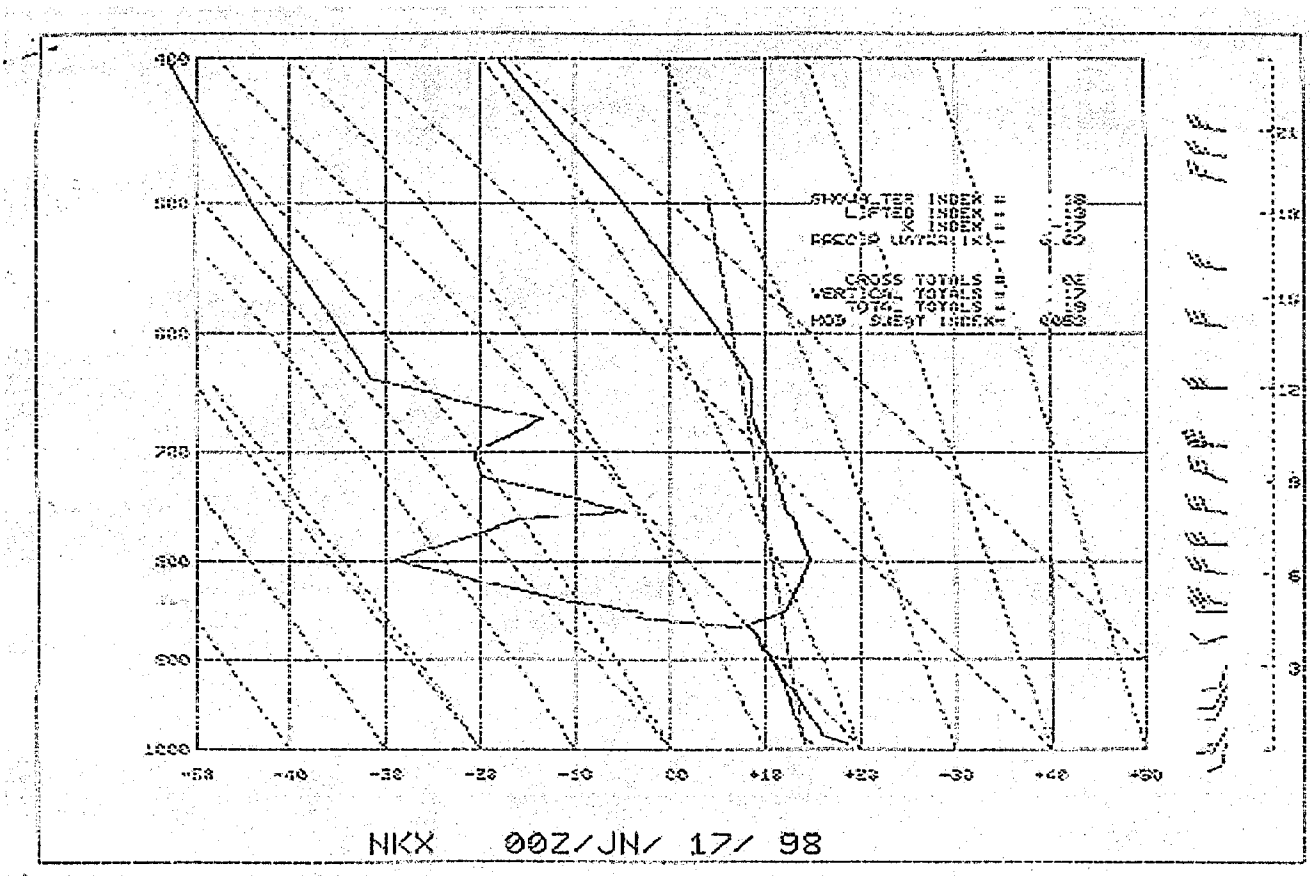

Fig. 6c. 0000 UTC 17 June 1998 NKX raob.

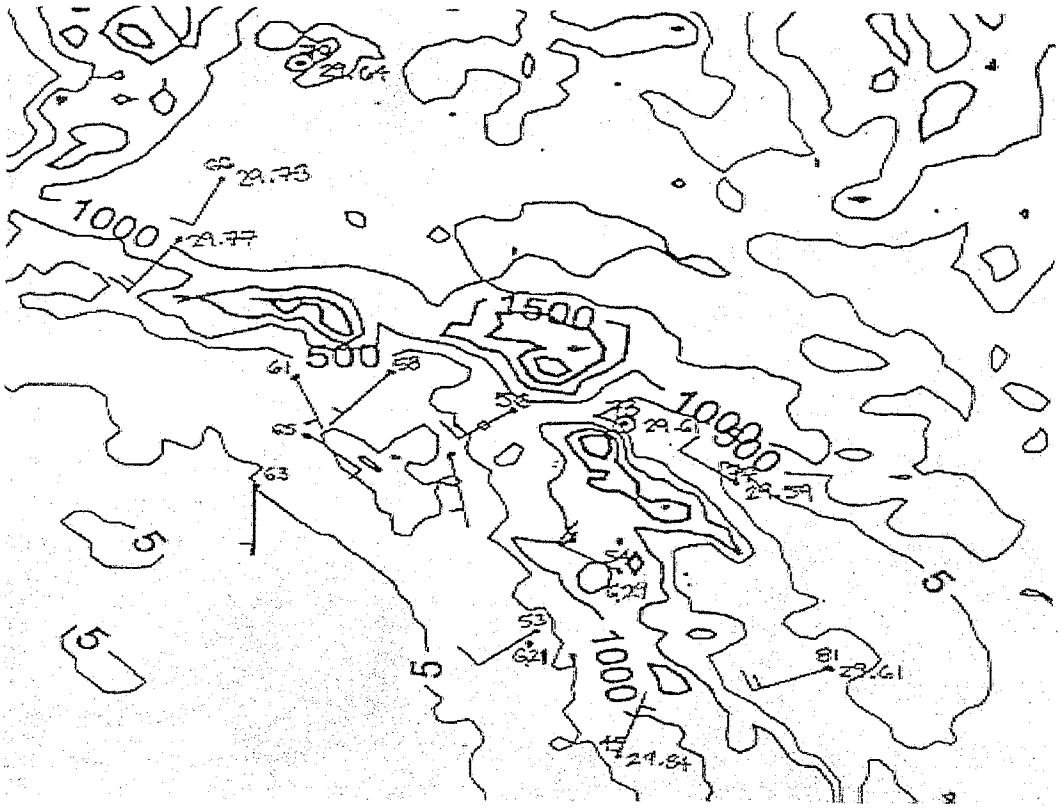

Fig. 7a. 1200 UTC 16 June 1998 surface plot. Terrain contour heights in meters. Wind speeds in knots.

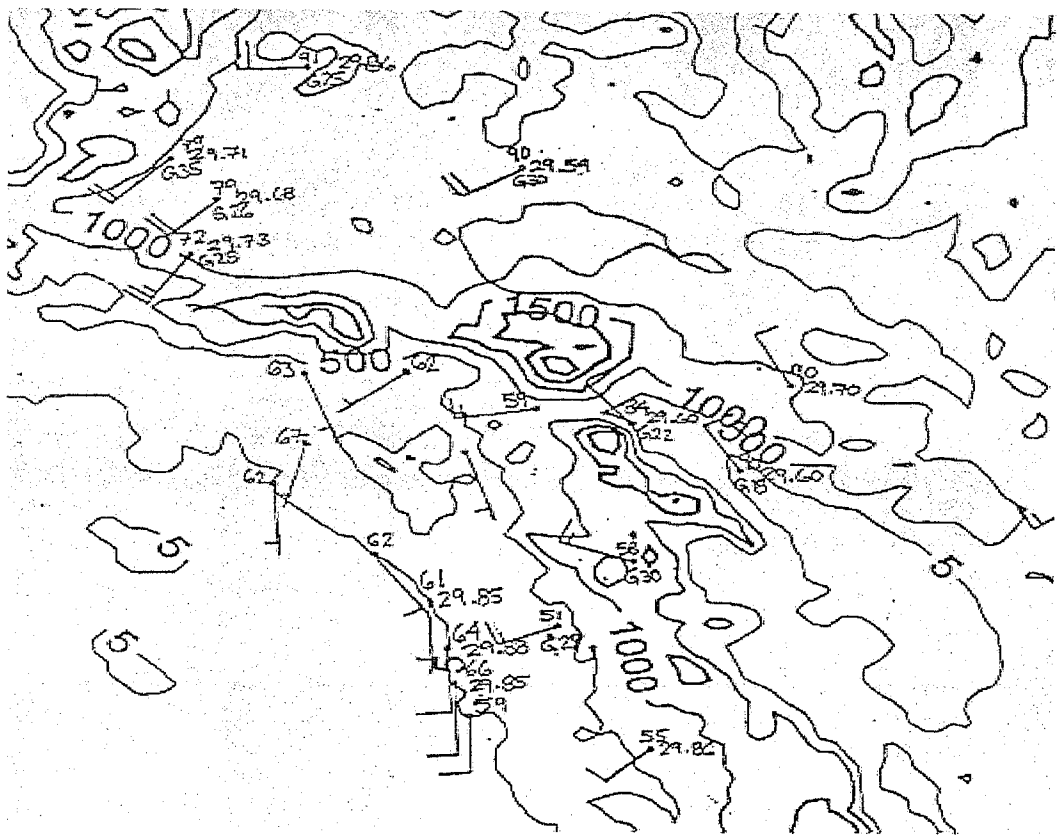

Fig. 7b. 1800 UTC 16 June 1998 surface plot. Terrain contour heights in meters. Wind speeds in knots.

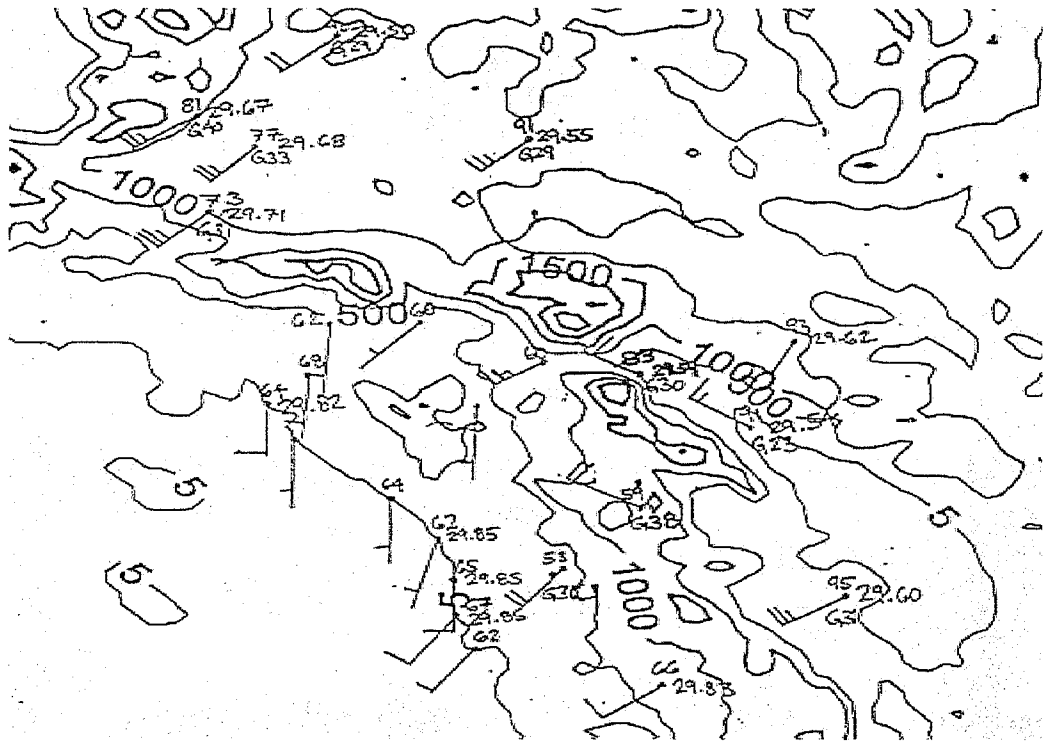

Fig. 8a. 2100 UTC 16 June 1998 surface plot. Terrain contour heights in meters. Wind speeds in knots.

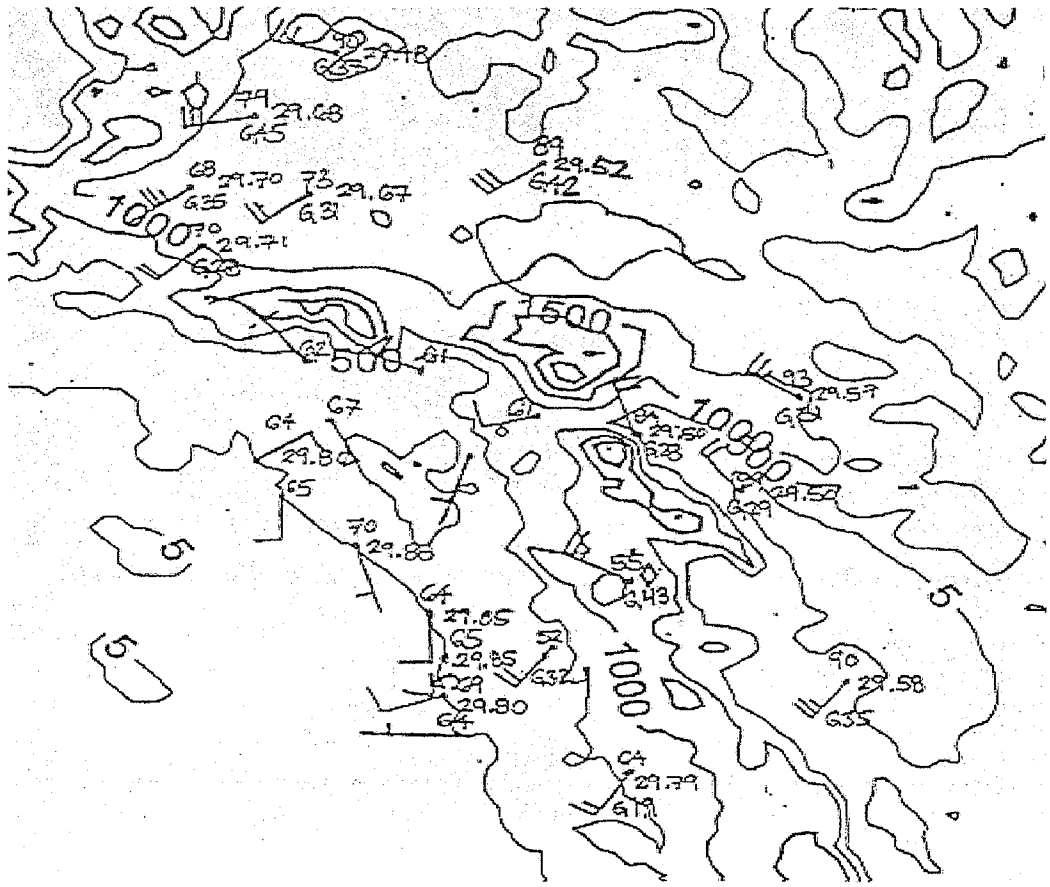

Fig. 8b. 0000 UTC 17 June 1998 surface plot. Terrain contour heights in meters. Wind speeds in knots.